

# Revised astrochronology for the Ain el Beida section (Atlantic Morocco): No glacio-eustatic control for the onset of the Messinian Salinity Crisis

W. Krijgsman<sup>1</sup>, S. Gaboardi<sup>2</sup>, F.J. Hilgen<sup>3</sup>, S. Iaccarino<sup>2</sup>, E. de Kaenel<sup>4</sup>, and E. van der Laan<sup>3</sup>

<sup>1</sup>Paleomagnetic laboratory "Fort Hoofddijk", Budapestlaan 17, 3584 CD Utrecht, The Netherlands

<sup>2</sup>Dip. di Scienze della Terra, Università di Parma, Parco Area della Scienze 1571A, 43100 Parma, Italy

<sup>3</sup>IPPU, Utrecht University, Budapestlaan 4, 3584 CD Utrecht, The Netherlands

<sup>4</sup>DPR, Matile 51, CH-2000 Neuchâtel, Switzerland

email: krijgsma@geo.uu.nl

---

**ABSTRACT:** Glacio-eustatic sea level lowering has often been proposed as a key mechanism for explaining the onset of the Mediterranean evaporites during the Messinian Salinity Crisis (MSC). To examine the role of glacio-eustasy during the progressive isolation of the Mediterranean in more detail, we reinvestigated the Ain el Beida quarry section that is located at the Atlantic margin of Morocco and therefore free of destructive MSC-related complications. The section consists of deep marine, cyclically bedded (reddish/beige), silty marls of late Messinian age. The reddish layers reveal the same characteristic signals as found in the Mediterranean sapropels (*Globigerinoides* spp. maxima and  $\delta^{18}\text{O}$  minima), suggesting that they correspond to precession minima and, hence, (boreal) summer insolation maxima. We have established an integrated stratigraphy (calcareous plankton biostratigraphy, magnetostratigraphy, stable isotope stratigraphy and cyclostratigraphy) and an astronomical tuning of the Ain el Beida section by using conventional techniques and calibration methods. The astronomical ages for the biostratigraphic events and paleomagnetic reversals are in good agreement with the Mediterranean chronology, and confirm our cyclostratigraphic correlations. Stable isotope analyses reveal that the peak glacial stages TG22 and TG20 clearly post-date the initiation of the Messinian evaporites in the Mediterranean and that there is no evidence for a glacio-eustatic control for the onset of the MSC. Only the TG12-11 transition seems to correspond to a major intra-MSC event, i.e. the beginning of the Upper Evaporites. The typical Lago Mare facies of the Upper Evaporites was thus deposited during warmer climate conditions and associated higher global sealevel stands.

---

## INTRODUCTION

Ever since the discovery of thick Messinian evaporites all over the Mediterranean sea floor (Hsü et al. 1973, Ryan 1973), scientific debate has been directed to the question if the so-called Messinian Salinity Crisis (MSC) had been initiated by regional tectonic activity in the Gibraltar area or by global glacio-eustatic sea level changes (Clauzon et al. 1996, Hodell et al. 1994, Hodell et al. 2001, Kastens 1992, Krijgsman et al. 1999a, Krijgsman et al. 1999b, Weijermars, 1988). This controversy was impossible to solve by using MSC sequences because in the Mediterranean Basin it is extremely difficult to distinguish tectonic from climatic signals. The geological record from the open ocean provides continuous Messinian sequences that are relatively free of tectonic activity and less seriously affected by the MSC (Hodell et al. 2001, Shackleton et al. 1995a). The sedimentary archives from the Atlantic Ocean should thus allow a successful study of the role of glacio-eustatic sea level on the major lithological changes of the MSC, provided that a high-resolution astronomical time frame for both the Mediterranean and the Atlantic Messinian is available.

Benson and coworkers inferred that the best place to study the sedimentary expression of the MSC in the ocean archives is on the Atlantic margin of Morocco, because the Rifian Corridor was thought to have been the final marine connection that exchanged waters between Mediterranean and Atlantic during the Miocene (Benson et al. 1991, Benson et al. 1995, Benson and Rakic-El Bied 1996, Hodell et al. 1989, Hodell et al. 1994). At-

lantic Morocco is one of the few areas in the world where a complete late Miocene marine succession can be studied on land. The sections and drill holes of the Bou Regreg valley, nearby Rabat, comprise a continuous stratigraphic sequence without the destructive effects of the MSC (Benson and Rakic-El Bied 1996, Benson et al. 1991). As a result, these marine deposits contain the complete history of climatic and paleoceanographic conditions during the Messinian and serve as important stratigraphic links between Mediterranean and deep sea sequences (Hodell et al. 1994). In addition, Benson et al. (1995) established an astronomical tuning for the late Messinian sediments of the Ain el Beida section using image analysis techniques in combination with signature template comparison. At that time, however, detailed correlations to the MSC events were still hampered by the absence of a high-resolution astrochronology for the Mediterranean pre-evaporite deposits.

Recently, an astronomical polarity time scale (APTS) has been developed for the Mediterranean Messinian (Hilgen and Krijgsman 1999, Krijgsman et al. 1999a, Krijgsman et al. 2001) and astronomical ages were obtained for nine major Mediterranean planktonic foraminiferal events and all the Messinian paleomagnetic reversals (Hilgen et al. 1995, Krijgsman et al. 1999a, Sierro et al. 2001). The astronomical ages for the magnetic reversals are in good agreement with ages derived from sea floor spreading rates (Krijgsman et al. 1999a) and with the astrochronology for the South Atlantic (Shackleton and Crowhurst 1997). However, significant discrepancies exist –

also for biostratigraphic events – with the astrochronology of the Ain el Beida section (Benson et al. 1995). These discrepancies might be related to the image analysis technique used by Benson et al. (1995) instead of the more conventional tuning methods, because the astrochronology of the nearby but older Oued Akrech section proved to be in excellent agreement with the Mediterranean record (Hilgen et al. 2000).

The discrepancies in the astronomical ages hamper a straightforward and detailed comparison between the Mediterranean and open ocean records. For this reason, we have decided to re-study the Ain el Beida quarry section using similar techniques as in the Mediterranean sections. In this paper, the astronomical ages for all sedimentary cycles, bioevents and paleomagnetic reversals of Ain el Beida are obtained by tuning the characteristic sedimentary cycle patterns to the 65° Nlat summer insolation curve of the Laskar et al. (1993) and (2003) solutions, thus allowing us to evaluate the synchronous and diachronous nature of bioevents in the Atlantic and Mediterranean records. Furthermore, the benthic oxygen isotope record of Ain el Beida can be compared with the Mediterranean event stratigraphy to investigate the possible relation between glacio-eustatic sea level changes and the onset of the MSC. The astronomical tuning of the Ain el Beida section will in addition provide the high-resolution age model necessary for detailed paleoclimatic and paleoceanographic studies directed at the stability of phase relations.

## BACKGROUND STUDIES

The Ain el Beida section is located in a brick quarry along the Bou Regreg river, a few kilometres south of Rabat (text-fig. 1). It consists of deep marine, cyclically bedded, silty marls of late Miocene age, which are locally referred to as the “Blue Marls” as they appear when freshly exposed. The first studies of Ain el Beida dealt with the planktonic foraminiferal biostratigraphy of the Moroccan Neogene (Feinberg and Lorenz 1970, Wernli 1977). Cita and Ryan (1978) were the first to investigate the section in search of the sedimentary expression of the MSC outside the Mediterranean. Moreover, they already noticed the correlation potential of the sedimentary cyclicity, which they interpreted to have a climatic origin.

The stratigraphic importance of the Bou Regreg area significantly increased with the drilling of long cores at Ain el Beida and Salé, allowing a detailed study of the entire stratigraphic interval between 7.5 and 4.4 Ma (Benson et al. 1991, Hodell et al. 1994). Planktonic and benthic foraminifera, calcareous nannofossil, and ostracod studies have resulted in a detailed biostratigraphic frame for the Messinian of Atlantic Morocco, although discrepancies exist in the location of several biostratigraphic events between Ain el Beida and Salé (Benson et al. 1991, Benson et al. 1995, Benson and Rakić-El Bied 1996, Hodell et al. 1989, Hodell et al. 1994). The paleomagnetic signal is reported as very good in the fresh drill cores and sufficiently strong in the outcrops (Benson et al. 1995, Hodell et al. 1994). Consequently, the magnetic polarity sequences of both Ain el Beida and Salé allow a straightforward correlation to the geomagnetic polarity time scale (GPTS). Oxygen isotope studies display regular variations with an estimated period of 40 kyr and are interpreted to reflect changes in global ice volume caused by obliquity-induced (41 kyr) changes in solar insolation at high latitudes (Hodell et al. 1994). By contrast, the basal sedimentary cyclicity was inferred to reflect the climatic precession signal (19 and 23 kyr) and was used to establish an astronomical tuning for the Ain el Beida section (Benson et al.

1995). Finally, Benson and Rakić-El Bied (1996) have proposed the Ain el Beida section as the Global Stratotype Section and Point (GSSP) of the Pliocene, but this was never accepted. The boundary has recently been formally defined at the base of the Trubi Formation in the Eraclea Minoa section of Sicily at 5.33 Ma (Van Couvering et al. 2000).

## INTEGRATED STRATIGRAPHY OF AIN EL BEIDA

### Cyclostratigraphy

Color cycles in the Ain el Beida section consist of regular alternations of indurated light beige colored marls and softer, more clayey and reddish colored marls. Apart from measuring bedding thickness, a visual distinction was made, on a scale from 1 to 10, in the color intensity of the reddish layers (text-fig. 2). In addition to the field observations, the color of the collected samples was measured with a Minolta CM-508I spectrophotometer. The resulting red-green component (a-values) of the color records, which were measured on both wet and dry samples, match the cyclicity observed in the field (text-fig. 3).

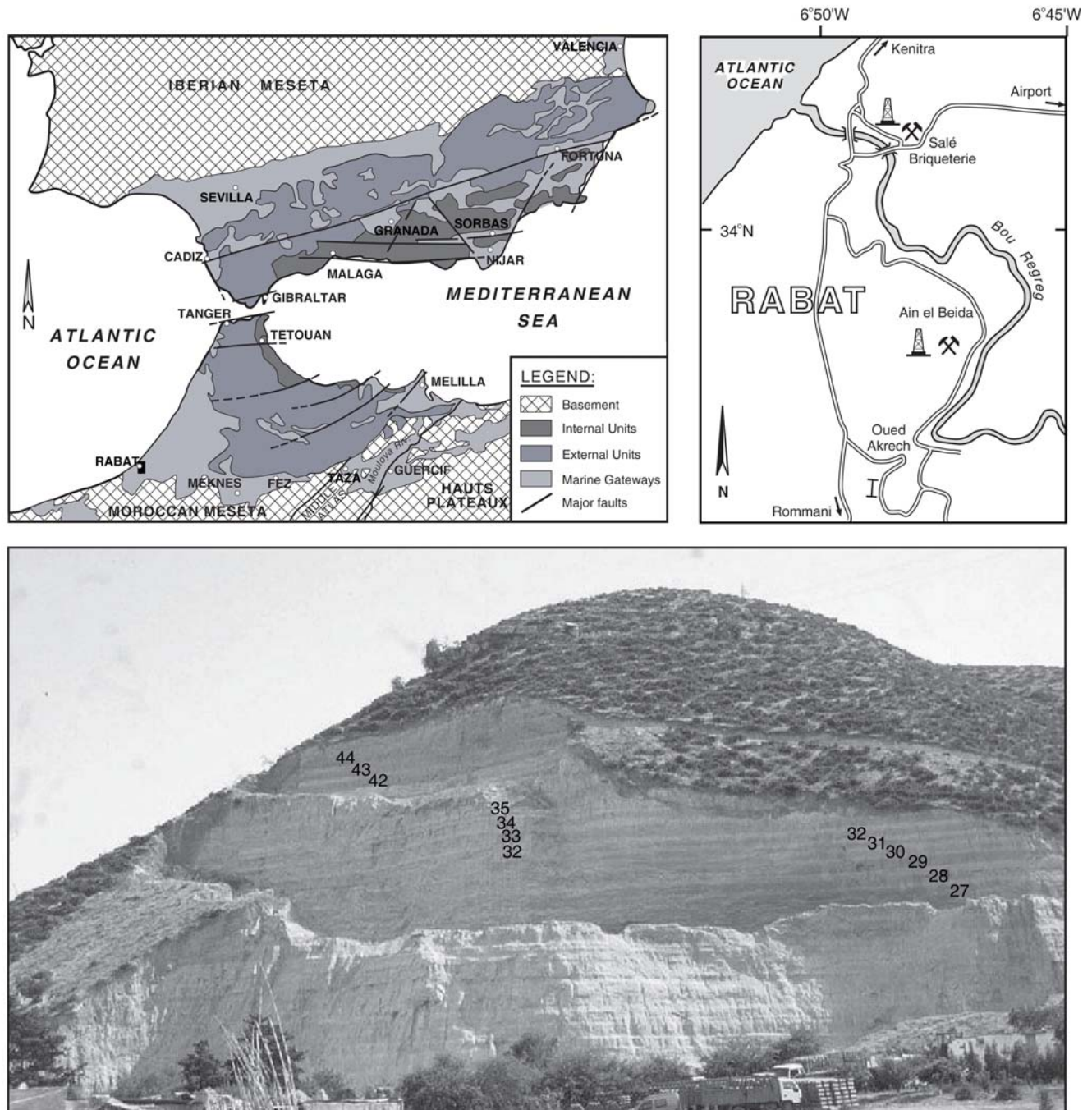
In total 44 cycles were recognized at Ain el Beida. The thickness of the cycles ranges from 60–350 cm with an average thickness of 165 cm. The interval between cycles AEB 34 and AEB 42 is the most difficult part of the section, lithological color variations are less distinct, thus complicating the determination of the exact number of cycles. The reddish colored marls, and to a lesser extent the beige marls, reveal marked changes in thickness alternations of thicker and thinner beds in successive cycles (AEB 15–23). Intervals in which the contrast between red and beige marls is conspicuous, alternate with intervals of less distinct variations. Thick and prominent reddish layers usually reappear every five basic sedimentary cycles (AEB 9, AEB 13/14, AEB 19, AEB 23, AEB 28/29, AEB 33/34, AEB 38, AEB 42/43/44). Intervals marked by thicker and more prominent reddish layers can also be distinguished on a larger scale. These intervals (AEB 8–13, AEB 27–34 and AEB 42–44) contain 7 or 8 cycles but this number increases to slightly less than 20 when the less distinct cycles below or above are included in the count as well. This 1:5:20 ratio is commonly observed in sedimentary records where both precession and eccentricity play a role.

### Biostratigraphy

#### Planktonic foraminifera

Micropaleontological analysis started with counting all planktonic foraminifera in the >125 µm fraction of 297 samples processed at the Department of Earth Sciences in Parma. Per sample, 250–300 specimens were counted in splits (using an Otto microsampler) and identified at the species level. Preservation is generally good and on average better in the reddish than in the beige layers. The detrital component is generally poor. The low number of foraminiferal fragments (more common in the beige layers) excludes dissolution effects, while the number of undeterminable specimens is related to their small size, not to bad preservation. The planktonic foraminiferal biostratigraphy is based on the qualitative and quantitative records of several marker species, which allowed the recognition of the following events in stratigraphic order (text-fig. 2):

- 1) the sinistral to dextral coiling change of *Neoglobobulimina acostaensis*;
- 2) the *Globobulimina miotumida* last regular occurrence (LRO); and the *Globobulimina margaritae* first occurrence (FO);
- 3) the decrease of dextrally coiled *Globobulimina scitula*;
- 4) the base of the acme of *G. margaritae*;



TEXT-FIGURE 1

Simplified geological sketch map of the Gibraltar area (up left), showing the Bou Regreg area near Rabat in the context of the marine Atlantic-Mediterranean gateways during the late Miocene. The detailed map of the Bou Regreg area (up right) shows the location of the Ain el Beida quarry section, the Tortonian/Messinian GSSP section of Oued Akrech, and the Salé quarry. The photograph of the Ain el Beida section (down), is taken several years after our sampling campaign in 1996. The quarry phase is constantly changing due to ongoing excavations. Numbers in the picture correspond to AEB cycles.

5) the top of the acme of *G. margaritae*.

The same events were recognized earlier by Sierro et al. (1993) and Benson et al. (1996) although a detailed comparison show significant differences which need some discussion.

The shift of *Neogloboquadrina* coiling was recognized earlier in the study area (Benson and Rakic-El Bied 1996, Bossio et al. 1976, Cita and Ryan 1978, Hodell et al. 1989), while Sierro et al. (1993) recognized the same event (their PF-Event 4) in the NE Atlantic, the North Betic and South Rifian gateways, and the western Mediterranean. The sharp shift from sinistral to

dextral coiling of *N. acostaensis* in cycle AEB 6 is followed, however, by 12 more or less pronounced sinistral influxes, most of them located in the interval between AEB 11 to AEB 32 (text-fig. 2). Benson et al. (1995) only recognized 7 influxes, which is most likely related to a lower sample resolution. These influxes are commonly confined to the beige layers, apart from the influxes in AEB 20 and AEB 21, which include the red layer of cycle AEB 20.

*Globorotalia margaritae* is initially very rare and shows a regular increase in abundance to the upper part of the section where the *G. margaritae* acme is situated (text-fig. 2). The base of the acme at 43 metres is coincident with a decrease in *Globorotalia juanai*. This event should be equated with PF-Event 6, although it occurs at a much higher level above PF-Event 5 than reported by Sierro et al. (1993). Moreover, the top of the acme in the uppermost part of the section does not correspond to a real drop in abundance, as this taxon is still common in the Pliocene (Benson and Rakic-El Bied 1996).

The *Globorotalia miotumida* group shows a distribution pattern characterised by a sharp decrease and last regular occurrence (LRO) in AEB 8, which coincides with the *G. margaritae* FO. This event directly postdates the sinistral to dextral coiling of *N. acostaensis* (text-fig. 2) and closely corresponds to PF-Event 5 (Sierro et al. 1993). Higher in the section, the *G. miotumida* group is very rare and randomly distributed up to AEB 42, where a second influx occurs.

*Globorotalia scitula* is dominantly dextral throughout the section, but from the middle part (39 metres) upward dextral forms decrease and sinistral specimens become more abundant. This decrease corresponds to PF-Event D that Sierro et al. (1993) consider useful for Atlantic-Mediterranean correlations.

Finally, *Globoquadrina altispira* is common in the lower part of the section, becomes rare upward, but is common again in the uppermost part. *Sphaeroidinellopsis* is regularly present throughout the section but is never common.

#### Calcareous nannofossils

The standard calcareous nannofossil biostratigraphy for the Messinian only comprises two bioevents, the *Amaurolithus primus* and/or *Amaurolithus delicatus* FO and the *Discoaster quinqueramus* LO (Martini 1971, Okada and Bukry 1980). In the present study, an attempt is made to determine additional biohorizons and bioevents to improve the biostratigraphic resolution of the late Messinian. A total of 297 samples were processed in the laboratory of DeKaenel Paleo Research (DPR) in Neuchâtel, Switzerland, using the settling methodology reported in De Kaenel and Villa (1996). This settling technique uses a constant volume of sediment, and provides a uniform dispersion of calcareous nannofossils on each slide. Preservation is generally very good and abundance and diversity are very similar between the reddish and beige layers. The results reveal eight important events (text-fig. 2):

- a) the top of an acme zone of *Discoaster quinqueramus*;
- b) the *Amaurolithus amplificus* last regular occurrence (LRO) and the *Calcidiscus macintyreii* (>11µm) first regular occurrence (FRO);
- c) the *Discoaster quinqueramus* LCO;
- d) the *Amaurolithus amplificus* LO and the *Cryptococcolithus mediaperforatus* LCO;
- e) the *Discoaster neorectus* (>20µm) LO;
- f) the *Discoaster quinqueramus* (>20µm) LO;

- g) the *Discoaster surculus* FCO;
- h) the *Discoaster quinqueramus* LO;

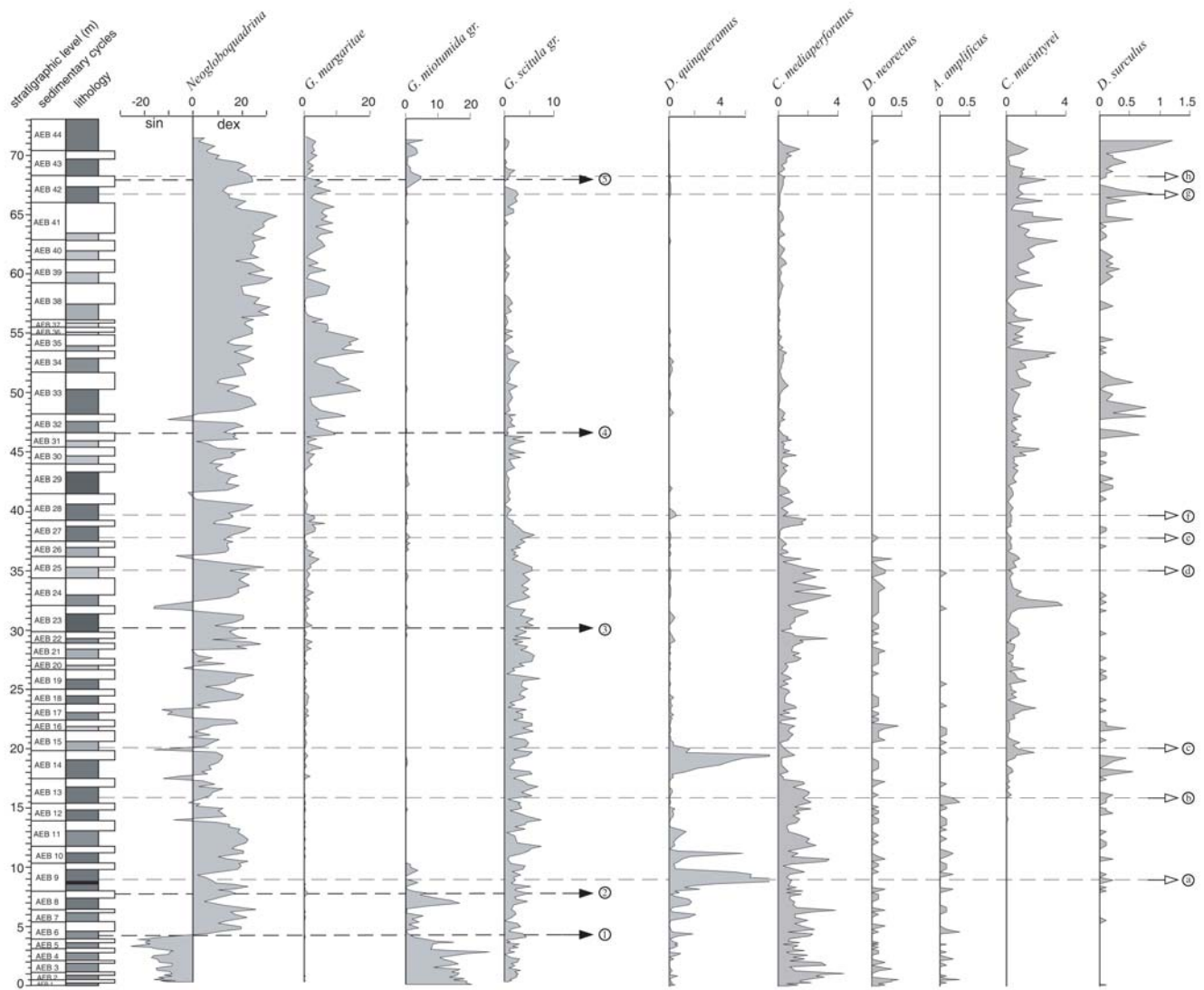
The top of an acme zone of *D. quinqueramus* (text-fig. 2; only specimens with a prominent knob were included) is recorded in the reddish layer of AEB 9 and is marked by a drop in abundance from 11 specimens per mm<sup>2</sup> to 6 specimens per mm<sup>2</sup>. This acme is not related to dissolution. The *D. quinqueramus* LCO is marked by the last important drop in abundance from 9 to 1.6 specimens per mm<sup>2</sup> and finally to 0.3 specimens per mm<sup>2</sup> and is recorded in the reddish layer of AEB 15 (text-fig. 2). Rakic el Bied and Benson, (1996) recorded this event in Ain el Beida at an older level, directly following the sinistral to dextral coiling change of *Neogloboquadrina acostaensis*. The abundance of *D. quinqueramus* in the upper part of its range is very low, especially when compared to the records of the western Atlantic Ocean (Backman and Raffi 1997). Nevertheless, even this weak distribution pattern provides some clear biostratigraphic signals. The *D. quinqueramus* (>20µm) LO corresponds to the *D. quinqueramus* LRO and occurs in the reddish layer of AEB 28. The *D. quinqueramus* LO, which is used in most biostratigraphic zonal schemes, occurs at the boundary between AEB 42 and AEB 43. Rakic el Bied and Benson (1996) recorded this event at a much older level (in C3An.1n). According to them, this event predates the *Globorotalia miotumida* LO and postdates the main sinistral to dextral coiling change of *Neogloboquadrina acostaensis*.

*Amaurolithus amplificus* is rare but consistently recorded within the lower part of the section up to AEB 13. The *A. amplificus* LRO coincides with the *C. macintyreii* (>11µm) FRO and occurs in the reddish layer of AEB 13 (text-fig. 2). The *A. amplificus* LO is recorded in the reddish layer of AEB 25. The *A. amplificus* LO has been recognized in different oceans (e.g. Backman and Raffi 1997, Gartner 1992, Mazzei et al. 1979, Raffi and Flores 1995, Rio et al. 1990).

The *C. macintyreii* (>11µm) FRO corresponds to the recurrence of morphotypes larger than 11µm (morphotype A of Knappertsbusch (2000)). Very often, *C. macintyreii* (>11µm) is not recorded in the lower part of the Messinian, but reoccurs in the upper part. A similar absence interval was observed for *Reticulofenestra pseudoumbilica* (>7µm) (Gartner 1992, Raffi and Flores 1995, Rio et al. 1990). Young (1990) and Takayama (1993) described several late Miocene "small *Reticulofenestra* intervals" that can be correlated between the Atlantic, Indian and Pacific Oceans. The same sequential size variations are found in the genus *Calcidiscus* (Knappertsbusch 2000).

*Cryptococcolithus mediaperforatus* is continuously present throughout the section (its LO is a lower Pliocene event). The abundance pattern of *C. mediaperforatus* (text-fig. 2) represents only forms larger than 5µm. Smaller forms have been counted separately. The *C. mediaperforatus* LCO corresponds to a drop in abundance from 2.8 specimens per mm<sup>2</sup> to 0.3 specimens per mm<sup>2</sup> and is located in the reddish layer of AEB 25.

*Discoaster neorectus* (text-fig. 2; only specimens larger than 20 µm are counted) is present in low but consistent abundances up to 37.82 m (0.1 mm<sup>-2</sup> corresponds to 1 specimen per two long traverses on a slide) where the *D. neorectus* LO occurs in the reddish layer of AEB 27. Smaller specimens (up to 17µm) are present to the top of the section. Because *D. neorectus* is rare, its occurrence is often not reported in published nannofossil range charts. Nevertheless, the *D. neorectus* (>20µm) LO is used as a secondary marker species to define the top of the *Discoaster*



TEXT-FIGURE 2

Cyclostratigraphy and calcareous plankton biostratigraphy of the Ain el Beida section. In the lithological column a distinction was made in the color intensity of the reddish layers on a scale from 1 to 10. Quantitative distribution patterns of planktonic foraminiferal and calcareous nannofossil (horizontal nannofossil scale is in specimens/mm<sup>2</sup>) marker species and the position of the main events: Planktonic foraminifera - 1) Main sinistral to dextral coiling change of *Neogloboquadrina acostaensis*; 2) *Globorotalia miotumida* last regular occurrence (LRO) and *Globorotalia margaritae* first occurrence (FO); 3) decrease of dextrally coiled *Globorotalia scitula*; 4) base of *G. margaritae* acme; and 5) top of *G. margaritae* acme. Calcareous nannofossils - a) top of *Discoaster quinqueramus* acme; b) *Amaurolithus amplificus* last regular occurrence (LRO) and *Calcidiscus macintyreii* (>11 μm) first regular occurrence (FRO); c) *Discoaster quinqueramus* LCO; d) *Amaurolithus amplificus* LO and *Cryptococcolithus mediaperforatus* LCO; e) *Discoaster neorectus* (>20 μm) LO; f) *Discoaster quinqueramus* (>20 μm) LO; g) *Discoaster surculus* FCO; and h) *Discoaster quinqueramus* LO. The stratigraphic position (and ages) of the events is summarized in Table 2.

*neorectus* Subzone (Bukry 1973). At Ain el Beida, *D. neorectus* occurs up to the *Amaurolithus primus* Subzone. This higher occurrence of *D. neorectus* has also been observed in the Atlantic Ocean where it was reported above the *A. delicatus* FO at the level of the *D. berggrenii* LO (Gartner 1992).

*Discoaster surculus* is rare and discontinuously present in the lower part of the section but becomes more common and continuously present in the upper part. The FCO of *D. surculus* occurs in the uppermost part of the section at cycle AEB 42 and is placed at an increase in abundance from 0.1 to 0.8 specimens per mm<sup>2</sup>.

Furthermore, several additional bioevents have been recognized which include: 1) the *Discoaster calcaris* LO in the reddish layer of AEB 1, 2) the *Reticulofenestra rotaria* (>5 μm) LCO in the reddish layer of AEB 3 where its abundance drops from 4 specimens per mm<sup>2</sup> to 0.4 specimens per mm<sup>2</sup>, 3) the top of an acme zone of *Discoaster brouweri* at the top of the beige layer of AEB 5, 4) the top of an acme zone of the Scyphosphaera group at the top of the reddish layer of AEB 10, 5) the *Discoaster berggrenii* LO between the reddish and beige layers of AEB 34, 6) the *Helicosphaera orientalis* LO between AEB 37 and AEB 38, 7) the *Helicosphaera stalis ovata* LO between AEB 38 and AEB 39, 8) the *Helicosphaera stalis stalis* last occurrence datum (LOD) between the reddish and whitish layers

of AEB 42, 9) the *Triquetrorhabdulus rugosus* LOD between the reddish and the whitish layers of AEB 43, and 10) the *Reticulofenestra rotaria* (>5 $\mu$ m) LO at the base of the reddish layer of AEB 44.

### Magnetostratigraphy

The freshly excavated sediment in the basal part of the Ain el Beida quarry shows the characteristic blue color, which rapidly changes (within days) to beige/reddish when exposed to air. This suggests that secondary haematite is formed within the sediment through weathering by chemical alteration (oxidation) of primary iron minerals like magnetite or iron sulfides. Hence, it may be expected that secondary overprints may significantly disturb the paleomagnetic signal. Therefore, thermal demagnetization is applied with small temperature increments of 20-50°C up to a maximum temperature of 600°C to discriminate the primary component of the magnetization. Paleomagnetic samples were taken from 247 levels with a water-cooled drill and oriented with a magnetic compass. The natural remanent magnetization (NRM) was measured on a 2G Enterprises DC SQUID cryogenic magnetometer in the paleomagnetic laboratory Fort Hoofddijk of the Utrecht University. Principal component analysis was applied to determine the component directions of the NRM, chosen by inspection of vector end-point demagnetization diagrams.

NRM intensities of the Ain el Beida section range between 0.5 and 2.5 mA/m and have an average value of approximately 1.0 mA/m. Thermal demagnetization results revealed Zijderveld diagrams of mixed quality (text-fig. 4). They generally show a randomly oriented viscous laboratory component, which is completely removed at temperatures of 100°C, and a low-temperature (LT) component of normal polarity that is demagnetized in the 100-240°C temperature range. This LT component is interpreted as a secondary present-day field component. Although the directions are slightly scattered, the average inclination of 51° for this present-day component closely coincides with the expected inclination of (53.5°) that corresponds to the latitude of Ain el Beida at 34°N (text-fig. 5). Progressive demagnetization in the 240-440°C temperature range revealed additional normal or reversed components in approximately 50% of the Zijderveld diagrams. This 240-440°C component is interpreted as the primary component or the characteristic remanent magnetization (ChRM). One sample (AEB 082; 21.73m) showed atypical demagnetization behaviour with a normal polarity component in the 240-400°C range, but with a clear reversed polarity component at higher temperatures. This sample is interpreted as reversed and presented in the magnetostratigraphy column as a possibly reversed interval (text-fig. 4h).

Reversed directions are interpreted as reliable when diagrams displayed a south/up component that showed a linear or scattered decay towards the origin (text-fig. 4a,b) or when diagrams showed a clear linear decay of a reversed component without a trend towards the origin (text-fig. 4c). In the latter case, it is assumed that another secondary component of normal polarity is present, but this component could not be properly demagnetized because heating towards temperatures higher than 440°C commonly resulted in the generation of a randomly oriented viscous component. Normal directions are only interpreted as reliable when diagrams displayed decay towards the origin in the 240-440°C temperature range (text-fig. 4d-f). Directions are qualified as unreliable when diagrams only show a cluster at temperatures higher than 240° (text-fig. 4g) or when directions are so scattered that a reliable interpretation is impossible.

Declinations and inclinations were calculated for each characteristic component stable endpoint direction. The ChRM directions and polarity zones show that three polarity reversals are recorded (text-fig. 3). Normal polarity intervals that only comprise one or two samples may correspond to short cryptochrons but more likely represent samples with a stronger secondary overprint. The normal and reversed directions are perfectly antipodal (text-fig. 5) and pass the reversal test. The overall mean direction is: Dec=3°, Inc=43° (N=116; k=10;  $\alpha_{95}$ =4) which indicates that the area has not undergone any significant rotation. The clear E-W elongation in the distribution of directions (text-fig. 5) suggests that the inclination of the primary component has probably been reduced by sediment inclination error (Tauxe and Kent 2004, Krijgsman and Tauxe 2004).

### Stable Isotopes

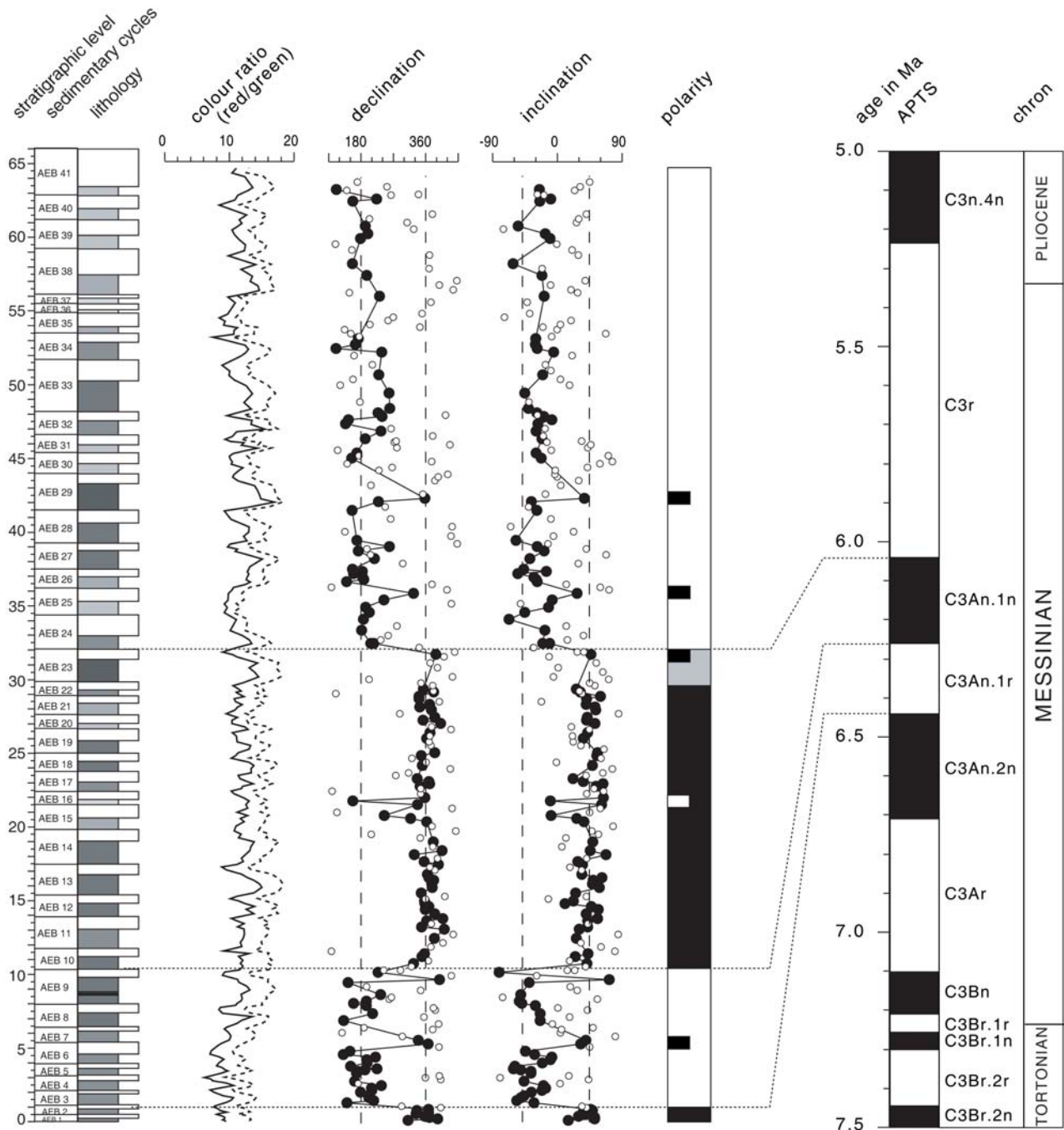
Oxygen isotope analysis was performed on the calcitic tests of the benthic foraminiferal species *Planulina ariminensis* which were picked from the >125 $\mu$ m fraction in 297 samples. All samples were processed in the laboratory of the Department of Earth Sciences in Utrecht and data are reported as per mil (‰) relative to the PeeDee belemnite (PDB) standard. For each sample, about twenty specimens of *P. ariminensis* were picked, yielding duplicate analyses for most samples. In order to remove any organic remains, each sample was roasted for 30 minutes at 470°C under vacuum. The samples were analyzed using an ISOCARB. This system is directly coupled to a mass spectrometer and has the capacity to measure 44 samples during a run, including 1 international (IAEA-CO-1), and 9 in-house (NAXOS) standards. Each sample reacted with 103% phosphoric acid (H<sub>3</sub>PO<sub>4</sub>) for 6 to 7 minutes at 90°C. The analytical precision and accuracy were determined by replicate analyses of samples and by comparison with the international standard. The relative standard deviations, analytical precision and accuracy were better than 0.1‰.

The benthic oxygen isotope record shows a close link to the lithology of Ain el Beida, with enrichments in  $\delta^{18}\text{O}$  generally occurring in the beige layers and depletions in the reddish layers (text-fig. 6). The amplitude of the  $\delta^{18}\text{O}$  variations is ~1.0‰ with values ranging from about 0.4 to 1.3‰. The recurrence of thicker and more distinct reddish layers is marked by prominent excursions to light  $\delta^{18}\text{O}$  values, while most of the prominent excursions to heavy values occur in the beige layers within such “clusters” of distinct reddish layers. Apparently, variations in  $\delta^{18}\text{O}$  are also present that are not related to lithology. These variations occur at intervals with a thickness of approximately two color cycles. The heaviest  $\delta^{18}\text{O}$  values are found in the beige layers of cycles AEB 33, AEB 35 and AEB 42 in the upper part of the section, although heavy values also occur in the beige layers of cycles AEB 19 and AEB 21 in the lower part of the section.

## ASTRONOMICAL DATING OF AIN EL BEIDA

### Astronomical origin of the sedimentary cycles

The standard procedure to establish an accurate and reliable astronomical tuning of any geological record involves a number of steps. First it has to be proven that the observed cyclicity is indeed astronomically controlled. This can be achieved by determining the periodicity of the cyclicity, which can be compared with the well-known periodicities of the astronomical cycles of precession (~20 kyr), obliquity (~40 kyr) and eccentricity (~100 kyr and ~400 kyr).

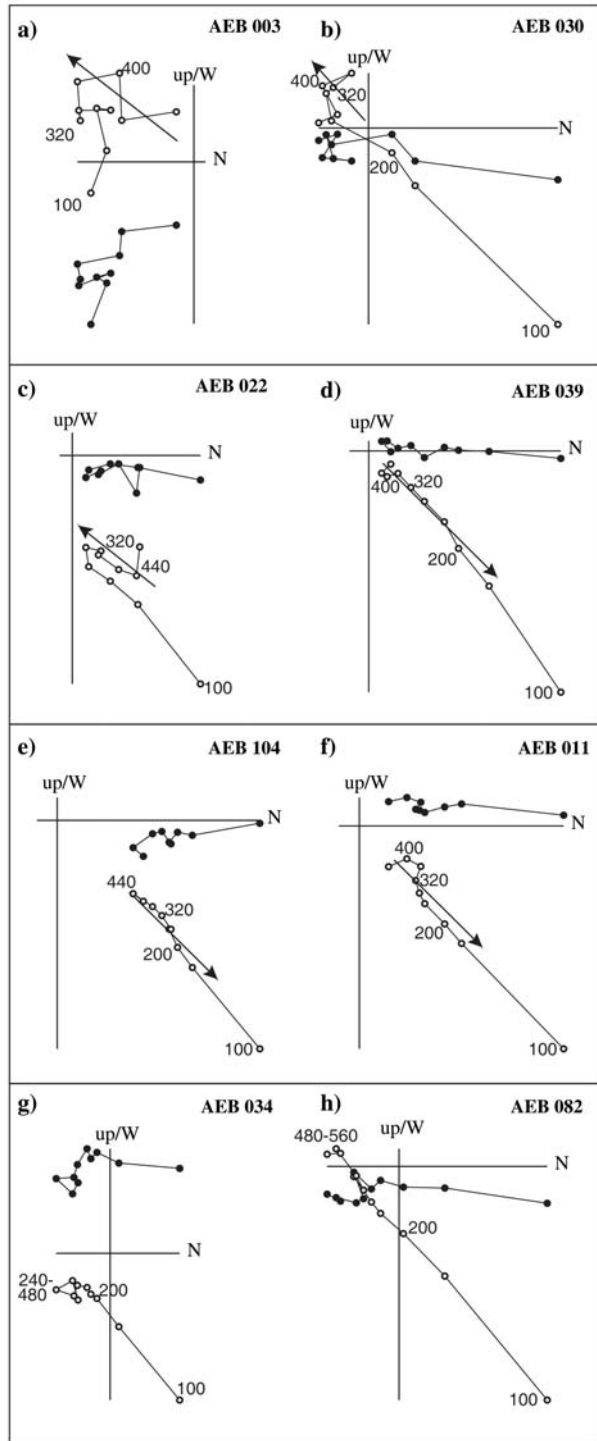


TEXT-FIGURE 3

Paleomagnetic and colour ratio data from the Ain el Beida section and correlation to the APTS. Solid (open) circles in the declination and inclination curves denote reliable (unreliable) results (see text for explanation). In the polarity column black (white) denotes normal (reversed) polarity intervals. The colour reflectance records (a-values) are measured and dry (solid line) and wet (dashed line) samples.

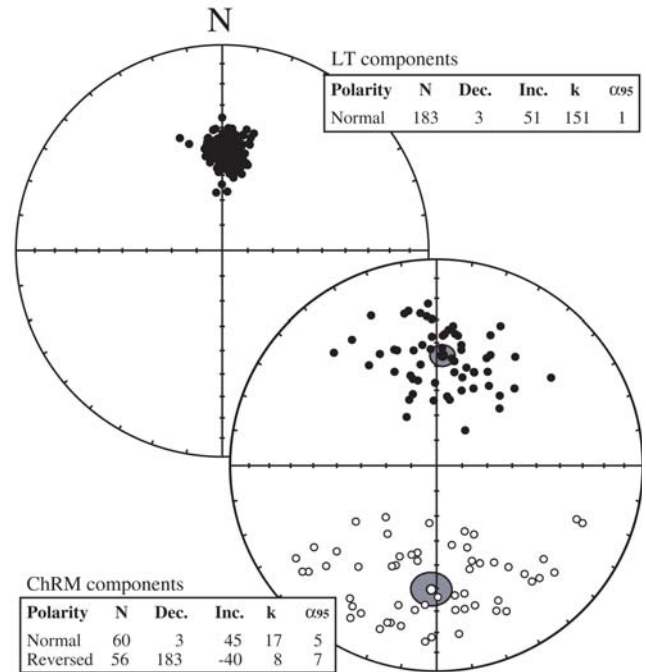
Biostratigraphic results from Ain el Beida confirm the late Messinian age of the section, as demonstrated by Benson et al. (1991; 1995), and indicate that the two complete magnetic intervals correspond to chrons C3An.1r and C3An.1n. These two intervals together comprise a total number of 20-21 sedimentary cycles, and correspond to 375 kyr according to the GPTS (Cande and Kent 1995) and to 400 kyr according to the APTS (Krijgsman et al. 1999a). The average periodicity of the basic

sedimentary cyclicity in Ain el Beida thus arrives at 18-19 kyr (GPTS) or 19-20 kyr (APTS), which is in good agreement with a precessional control. The same conclusion was reached by Benson et al. (1995) who determined the number of cycles from an image-processed photograph in their study of the sedimentary cycles at Ain el Beida. Independent confirmation of an astronomical origin of the cyclicity in the Blue Marls comes from the nearby Oued Akrech section. The integrated stratigraphic



TEXT-FIGURE 4  
Representative examples of thermal demagnetization diagrams from selected samples of the Ain el Beida section. Closed (open) symbols represent the projection of vector-end-points on the horizontal (vertical) plane; values indicate temperatures in degrees Celcius (°C).

results of Oued Akrech indicate that the basic cyclic alternation of indurated beige coloured marls and softer more clayey and reddish coloured marls is indeed dominantly precession-controlled (Hilgen et al. 2000).



TEXT-FIGURE 5  
Equal area diagrams showing the paleomagnetic directions of the secondary (LT) and the ChRM components. The 95% confidence ellipse for the normal and reversed mean directions is indicated. Statistical information: N, number of samples; Dec., declination; Inc., inclination; k, Fisher's precision parameter;  $\alpha_{95}$ , radius of the 95% confidence cone.

#### Phase relation with the astronomical cycles

The next step is the determination of the phase relation of the observed cyclicities with the orbital parameters. This is well known for the marine sequences of the Mediterranean Neogene where marl-sapropel cycles are precession controlled, with the sapropels corresponding to precession minima and summer insolation maxima. Detailed quantitative planktonic foraminiferal analyses and stable isotope records reveal characteristic sapropel signals with maxima in *Globigerinoides* spp. and minima in  $\delta^{18}\text{O}$  (Sprovieri et al. 1996). On a larger scale, sapropel clusters correspond to eccentricity maxima – both for the 100 and 400 kyr cycle – and intervals without, or with poorly developed, sapropels to eccentricity minima (Hilgen 1991). Maxima in eccentricity will enhance climate fluctuations on a precessional scale because eccentricity modulates the precession amplitude. Hence, it can be expected that eccentricity maxima will favour the formation of distinct cycles with strongly contrasting lithologies. By contrast, minima in eccentricity will result in intervals in which the cyclicity is poorly developed or absent. For different sedimentary environments, however, the astronomical origin of the cyclicity and the phase relation with the astronomical parameters needs to be determined before astronomical tuning can be established.

In the Ain el Beida section, the detailed quantitative planktonic foraminiferal analyses and stable isotope records reveal the same characteristic signal in the reddish layers as found in Mediterranean sapropels (*Globigerinoides* spp. maxima and  $\delta^{18}\text{O}$  minima). This implies that the reddish intervals are equivalents of sapropels in the Mediterranean and thus correspond to precession minima and insolation maxima. Moreover, Ain el Beida

TABLE 1

Stratigraphic position and astronomical ages of mid-points of red and beige marl beds of each color cycle in section Ain el Beida. The astronomical ages are based on the tuning shown in text-figure 5 and refer to ages of the correlative insolation maximum and precession minimum. Ages in regular style are based on tuning the color cycles to solution La93(1,1) and ages in italics are based on tuning the cycles to La2003(1,1).

Cycle	Lithol.	Insol.	Prec.	<i>Insol.</i>	<i>Prec.</i>	Cycle	Lithol.	Insol.	Prec.	<i>Insol.</i>	<i>Prec.</i>	Cycle	Lithol.	Insol.	Prec.	<i>Insol.</i>	<i>Prec.</i>
AEB15	beige	6.155	6.154	<i>6.154</i>	<i>6.153</i>	AEB30	beige	5.867	5.866	<i>5.866</i>	<i>5.864</i>	AEB44	red	5.520	5.520	<i>5.518</i>	<i>5.519</i>
	red	6.164	6.164	<i>6.163</i>	<i>6.163</i>		red	5.877	5.878	<i>5.876</i>	<i>5.876</i>		beige	5.531	5.530	<i>5.530</i>	<i>5.529</i>
	beige	6.174	6.174	<i>6.173</i>	<i>6.173</i>	AEB30	beige	5.888	5.888	<i>5.887</i>	<i>5.887</i>	AEB43	red	5.540	5.541	<i>5.539</i>	<i>5.540</i>
AEB14	red	6.184	6.184	<i>6.182</i>	<i>6.183</i>	AEB29	red	5.898	5.899	<i>5.897</i>	<i>5.898</i>		beige	5.551	5.551	<i>5.550</i>	<i>5.550</i>
	beige	6.196	6.195	<i>6.194</i>	<i>6.194</i>		beige	5.911	5.910	<i>5.909</i>	<i>5.908</i>	AEB42	red	5.561	5.561	<i>5.560</i>	<i>5.560</i>
AEB13	red	6.205	6.205	<i>6.204</i>	<i>6.204</i>	AEB28	red	5.919	5.920	<i>5.918</i>	<i>5.919</i>		beige	*	*	*	*
	beige	6.216	6.216	<i>6.215</i>	<i>6.215</i>		beige	5.930	5.930	<i>5.929</i>	<i>5.929</i>	AEB41	red	5.615	5.615	<i>5.613</i>	<i>5.614</i>
AEB12	red	6.226	6.227	<i>6.225</i>	<i>6.225</i>	AEB27	red	5.940	5.941	<i>5.939</i>	<i>5.940</i>		beige	5.626	5.625	<i>5.625</i>	<i>5.624</i>
	beige	6.239	6.238	<i>6.237</i>	<i>6.236</i>		beige	5.953	5.951	<i>5.952</i>	<i>5.951</i>	AEB40	red	5.635	5.635	<i>5.633</i>	<i>5.634</i>
AEB11	red	6.257	6.256	<i>6.256</i>	<i>6.248</i>	AEB26	red	*	5.961	<i>5.962</i>	<i>5.961</i>		beige	5.644	5.644	<i>5.643</i>	<i>5.643</i>
	beige	6.268	6.267	<i>6.267</i>	<i>6.266</i>		beige	*	5.965	<i>5.966</i>	<i>5.969</i>	AEB39	red	5.653	5.653	<i>5.652</i>	<i>5.653</i>
AEB10	red	6.277	6.278	<i>6.276</i>	<i>6.277</i>	AEB25	red	5.975	5.973	<i>5.974</i>	<i>5.971</i>		beige	*	*	*	*
	beige	6.289	6.288	<i>6.287</i>	<i>6.287</i>		beige	5.984	5.983	<i>5.983</i>	<i>5.982</i>	AEB38	red	5.691	5.691	<i>5.690</i>	<i>5.691</i>
AEB9	red	6.298	6.299	<i>6.297</i>	<i>6.297</i>	AEB24	red	5.993	5.994	<i>5.991</i>	<i>5.993</i>		beige	5.703	5.702	<i>5.702</i>	<i>5.701</i>
	beige	6.310	6.309	<i>6.309</i>	<i>6.308</i>		beige	6.004	6.004	<i>6.003</i>	<i>6.003</i>	AEB37	red	5.712	5.712	<i>5.711</i>	<i>5.711</i>
AEB8	red	6.319	6.320	<i>6.318</i>	<i>6.319</i>	AEB23	red	6.014	6.014	<i>6.013</i>	<i>6.013</i>		beige	5.722	5.722	<i>5.721</i>	<i>5.721</i>
	beige	6.330	6.330	<i>6.329</i>	<i>6.329</i>		beige	6.025	6.024	<i>6.024</i>	<i>6.023</i>	AEB36	red	5.733	5.733	<i>5.731</i>	<i>5.732</i>
AEB7	red	6.341	6.341	<i>6.340</i>	<i>6.340</i>	AEB22	red	6.033	6.034	<i>6.033</i>	<i>6.033</i>		beige	5.753	5.745	*	*
	beige	*	*	*	*		beige	6.043	6.043	<i>6.042</i>	<i>6.043</i>	AEB35	red	5.764	5.764	<i>5.764</i>	<i>5.763</i>
AEB6	red	6.373	6.372	<i>6.371</i>	<i>6.371</i>	AEB21	red	6.053	6.052	<i>6.052</i>	<i>6.052</i>		beige	5.774	5.774	<i>5.774</i>	<i>5.773</i>
	beige	6.383	6.383	<i>6.381</i>	<i>6.381</i>		beige	6.061	6.061	<i>6.061</i>	<i>6.061</i>	AEB34	red	5.784	5.785	<i>5.783</i>	<i>5.784</i>
AEB5	red	6.392	6.393	<i>6.391</i>	<i>6.391</i>	AEB20	red	6.069	6.070	<i>6.068</i>	<i>6.070</i>		beige	5.796	5.795	<i>5.795</i>	<i>5.794</i>
	beige	6.404	6.403	<i>6.402</i>	<i>6.402</i>		beige	6.080	6.080	<i>6.079</i>	<i>6.079</i>	AEB33	red	5.805	5.805	<i>5.804</i>	<i>5.804</i>
AEB4	red	6.413	6.413	<i>6.412</i>	<i>6.412</i>	AEB19	red	6.090	6.090	<i>6.089</i>	<i>6.089</i>		beige	5.817	5.816	<i>5.816</i>	<i>5.815</i>
	beige	6.423	6.423	<i>6.422</i>	<i>6.422</i>		beige	6.101	6.100	<i>6.099</i>	<i>6.099</i>	AEB32	red	5.826	5.827	<i>5.825</i>	<i>5.826</i>
AEB3	red	6.432	6.433	<i>6.431</i>	<i>6.432</i>	AEB18	red	6.110	6.111	<i>6.108</i>	<i>6.109</i>		beige	5.838	5.838	<i>5.837</i>	<i>5.837</i>
	beige	6.443	6.442	<i>6.443</i>	<i>6.442</i>		beige	6.121	6.121	<i>6.120</i>	<i>6.119</i>	AEB31	red	5.850	5.849	<i>5.848</i>	<i>5.848</i>
AEB2	red	6.451	6.451	<i>6.452</i>	<i>6.451</i>	AEB17	red	6.132	6.130	<i>6.130</i>	<i>6.129</i>						
	beige	6.459	6.46	<i>6.459</i>	<i>6.460</i>		beige	6.138	6.139	<i>6.138</i>	<i>6.138</i>						
AEB1	red	*	*	*	*	AEB16	red	6.145	6.146	<i>6.145</i>	<i>6.146</i>						

reveals several intervals in which the lithological expression of the cyclicity is enhanced (AEB 9, AEB 13/14, AEB 19, AEB 23, AEB 28/29, AEB 33/34 and AEB 42/43/44) suggesting that these intervals correspond to eccentricity maxima. Consequently, intervals in which the cyclicity is less distinct should correspond to eccentricity minima. The link between the reddish layers and precession minima/insolation maxima has also been suggested for the Oued Akrech section. For this section, only one calibration was possible when its persuasive thick-thin alternations are interpreted to reflect precession-obliquity interference (Hilgen et al. 2000). In contrast, the expression of the 100 kyr eccentricity cycle is almost completely lacking at Oued Akrech, which could be explained by the fact that the studied interval corresponds to a 2.35 Myr eccentricity minimum (Hilgen et al. 2000).

#### Astronomical tuning

To construct an independent astronomical tuning for the Ain el Beida section we refrain from using the Mediterranean-based astronomical ages for bioevents and paleomagnetic reversals. Nevertheless, all recent time scales indicate that the Ain el Beida section corresponds to the time interval between 6.5 and 5.5 Ma. The first order calibration involves the tuning to eccentricity. Intervals with distinct sedimentary cycles that contain prominent and thick reddish layers should correlate to eccentricity maxima while the interval of less distinct cycles should correspond to eccentricity minima. The most remarkable features in the eccentricity curve are the two suppressed 100-kyr eccentricity maxima at times of the 400 kyr eccentricity minimum around 5.6 Ma (text-fig. 6). Consequently, the interval

with less prominent sedimentary cycles (AEB 35-41) will correspond to the time interval between 5.8 and 5.6 Ma, when the maxima in 100 kyr eccentricity are reduced as a consequence of the 400 kyr minimum. Other possible correlations infer upward or downward shifts of 100 kyr. Evidently, these shifts make less sense because in those cases the well-developed cycles of AEB 33/34 or AEB 42/43/44 would then correlate with low amplitude eccentricity maxima where the lithological expression is expected to be less distinct.

The preferred first order correlation can furthermore be tested by the subsequent tuning of the basic sedimentary cycles to insolation. Between AEB 14 and 23 we observed nine more or less regularly developed cycles with cycles AEB 18 and 19 better developed and AEB 16 and 20 slightly less developed. This interval fits perfectly to the insolation curve interval between 6.0 and 6.2 Ma. Upward tuning is also in excellent agreement with the astronomical curve as the darker red layers of cycles AEB 23, 28/29, 33/34 and 38 nicely correspond to the highest amplitudes in insolation (text-fig. 6). The tuning of the upper part of the section is less straightforward. We expect that the well-developed cycles AEB 42/43/44 will correlate to the increase in amplitude above 5.6 Ma. This implies that the number of observed cycles is too low and that several low amplitude precession/insolation cycles lack sedimentary expression.

We started the tuning from the La93(1,1) solution (Laskar et al. 1993) with present-day values for dynamical ellipticity and tidal dissipation, hence (1,1), but repeated the whole tuning procedure for the new numerical solution La2003(1,1) (Laskar et al.

2003). This new solution has already been used to construct the new standard geological time scale for the Neogene (Lourens et al. 2004) and it is for this reason that we give the ages for the sedimentary cycles, calcareous plankton events and magnetic reversal boundaries according to both solutions in tables 1 and 2. As expected the application of the new solution does not change the tuning in a fundamental way and results in ages for the sedimentary cycles, calcareous plankton events and magnetic reversal boundaries that are only marginally different.

The tuning shows that the section comprises the time interval between 6.47 and 5.52 Ma and thus also the period during which the onset of evaporite deposition occurs in the Mediterranean: this onset is astronomically dated at  $5.96 \pm 0.02$  Ma (Krijgsman et al. 1999a). The astrochronology for the Ain el Beida section allows a detailed comparison of the AEB oxygen isotope record with the Mediterranean sequences, which can be used to investigate a possible glacio-eustatic control on the MSC events.

## DISCUSSION

### Astrochronology of Ain el Beida compared to the Mediterranean APTS

The astronomical tuning of Ain el Beida implies that the section can be correlated cyclostratigraphically on a bed-to-bed scale to the Mediterranean sections (text-fig. 7). The only two biostratigraphic events of Ain el Beida that are astronomically dated in the Mediterranean are the *s/d* coiling change in *N. acostaensis* and the *R. rotaria* LCO. The coiling change in *N. acostaensis* has frequently been recognized both in the Mediterranean and Atlantic and has an astronomical age of 6.361 Ma (e.g. Sierro et al. 2001) and references therein). Although it is often used for biostratigraphic purposes, this change took place at a time when neogloboquadrinids were extremely rare in the Mediterranean. Therefore, the first abundant occurrence of dextral *N. acostaensis* is considered a more reliable and easily identifiable event. This event has been recognized in sections from Spain, Italy and Greece (Hilgen and Krijgsman 1999, Krijgsman et al. 1999a; Sierro et al. 2001) and is astronomically dated at 6.339 Ma. In Ain el Beida, the neogloboquadrinids are more common and the recognized event thus relates to the real change in coiling from dominantly sinistral to dextral forms. The astronomical age of 6.373 Ma for the coiling change of *N. acostaensis* is in good agreement with ages for the same event in the Mediterranean record and suggests that the tuning of Ain el Beida is basically correct. The *s/d* coiling change in Ain el Beida is followed by twelve influxes of sinistral *N. acostaensis* which all occur in the beige layers, apart from the prolonged influx that covers the red layer of AEB 20 as well (text-fig. 2). In the Mediterranean, the coiling direction is dominantly dextral above the main *s/d* coiling change. This is not surprising because in the Mediterranean, neogloboquadrinids are absent in those parts of the sedimentary cycles that correspond to the beige marls of Ain el Beida (probably as a consequence of cyclically raised salinities in this pre-evaporitic part of the Mediterranean Messinian). The only exception is the single sinistral influx in the sapropel that corresponds to the red layer of AEB 20, again confirming the correctness of the tuning.

The *R. rotaria* LCO is recorded in the Metochia section on Gavdos (Greece) with an astronomical age of 6.940 Ma (Raffi et al. 2003), while our results reveal an age of 6.429 Ma (Table 1). An explanation for this discrepancy is that less favorable environmental conditions have decreased the abundance of *R.*

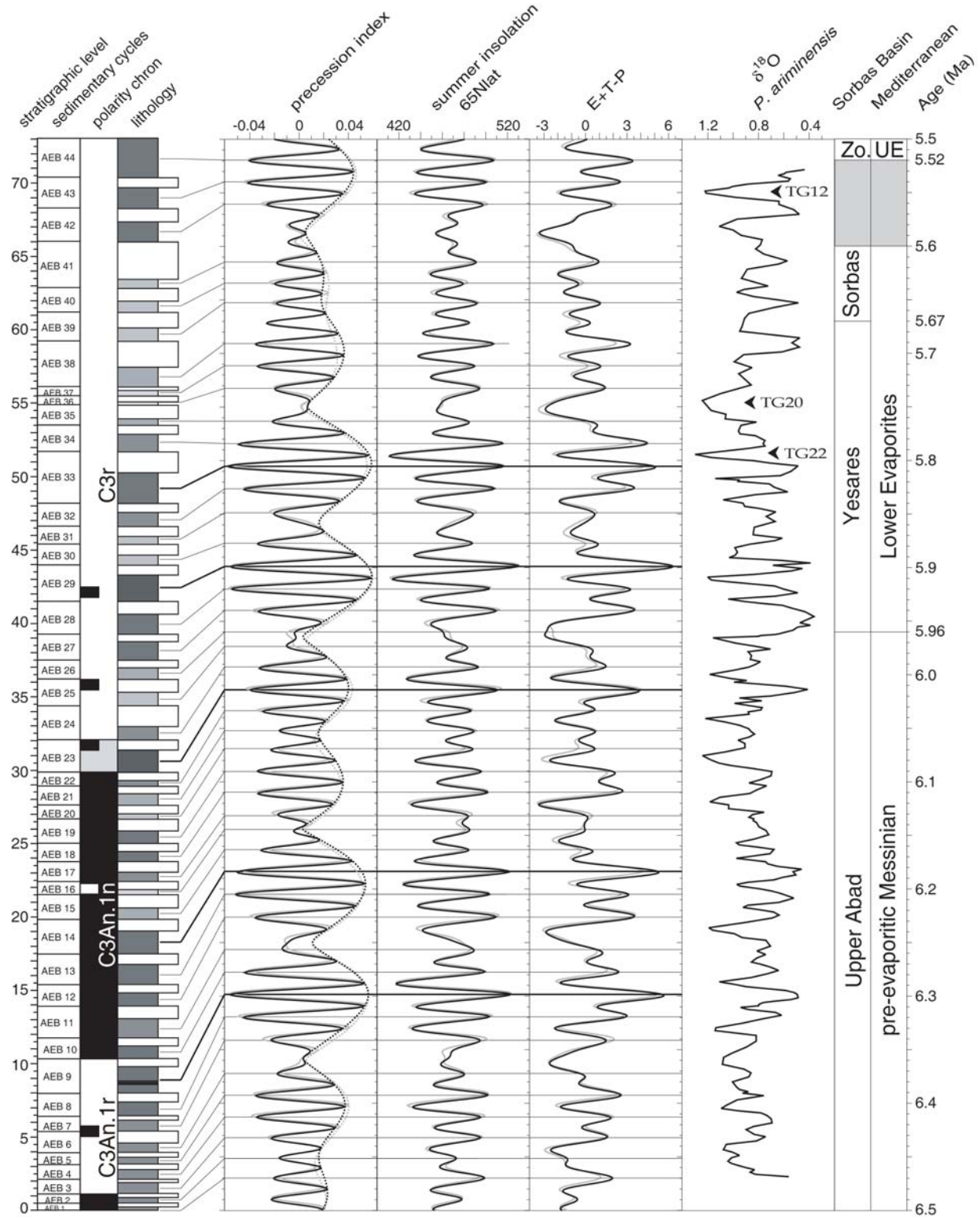
*rotaria* in the Mediterranean Sea and/or that several acme intervals may occur in the distribution pattern of *R. rotaria*. Raffi et al. (2003) identified an acme zone of *R. rotaria* in Metochia at about 6.4 Ma that corresponds with the LCO level at the AEB section. Therefore the *R. rotaria* (>5  $\mu$ m) LCO seems to be a reliable biostratigraphic event for correlations between the Mediterranean Sea and the Atlantic Ocean.

Benson et al. (1995) do not provide astronomical ages of biostratigraphic events so that we can only discuss their position relative to the magnetostratigraphic data. Our position of the main coiling change of *N. acostaensis* in the middle of the reversed chron C3An.1r is in good agreement with the results from Salé, but is reported from a younger level (lower part C3An.1n) at Ain el Beida by (Benson et al. 1995). Also in the Mediterranean and North Atlantic records this event falls within chron C3An.1r (Hodell et al. 2001, Krijgsman et al. 1999a, Sierro et al. 2001). The *G. margaritae* FO is reported by Benson et al. (1995) in both Ain el Beida and Salé at a much lower level (middle of C3An.2n) than in our record (upper part of C3An.1r). This can be explained by the limited downward extension of the Ain el Beida quarry section as compared with the Ain el Beida and Salé cores studied by Benson et al. (1991). Our position of the acme of *G. margaritae* (lower part C3r) is in good agreement with both the Ain el Beida and Salé records of Benson et al. (1995).

The astronomical ages for the paleomagnetic reversals in Ain el Beida are in good agreement with the ages determined in the Mediterranean Sorbas basin (Krijgsman et al. 1999a, Sierro et al. 2001). We have found the reversals at approximately the same stratigraphic level as Benson et al. (1995), as shown by the position of the bioevents and specific sedimentary cycles. However, the age for the reversals at Ain el Beida determined by the signature template technique (Benson et al. 1995) is clearly younger. The almost constant offset of ~100 kyr between the two dating techniques suggests that the image analysed record of Benson et al. (1995) was tuned to one eccentricity cycle younger. The ATS of Benson and co-workers is hampered by the fact that the number of sedimentary cycles does not match the number of precession cycles in the correlative interval of the orbital time series. Extraordinarily thick sedimentary cycles may represent double cycles, and thus explain the discrepancy in cycle numbers, but this adjustment will at the same time disrupt the characteristic cycle thickness pattern on which the tuning is based.

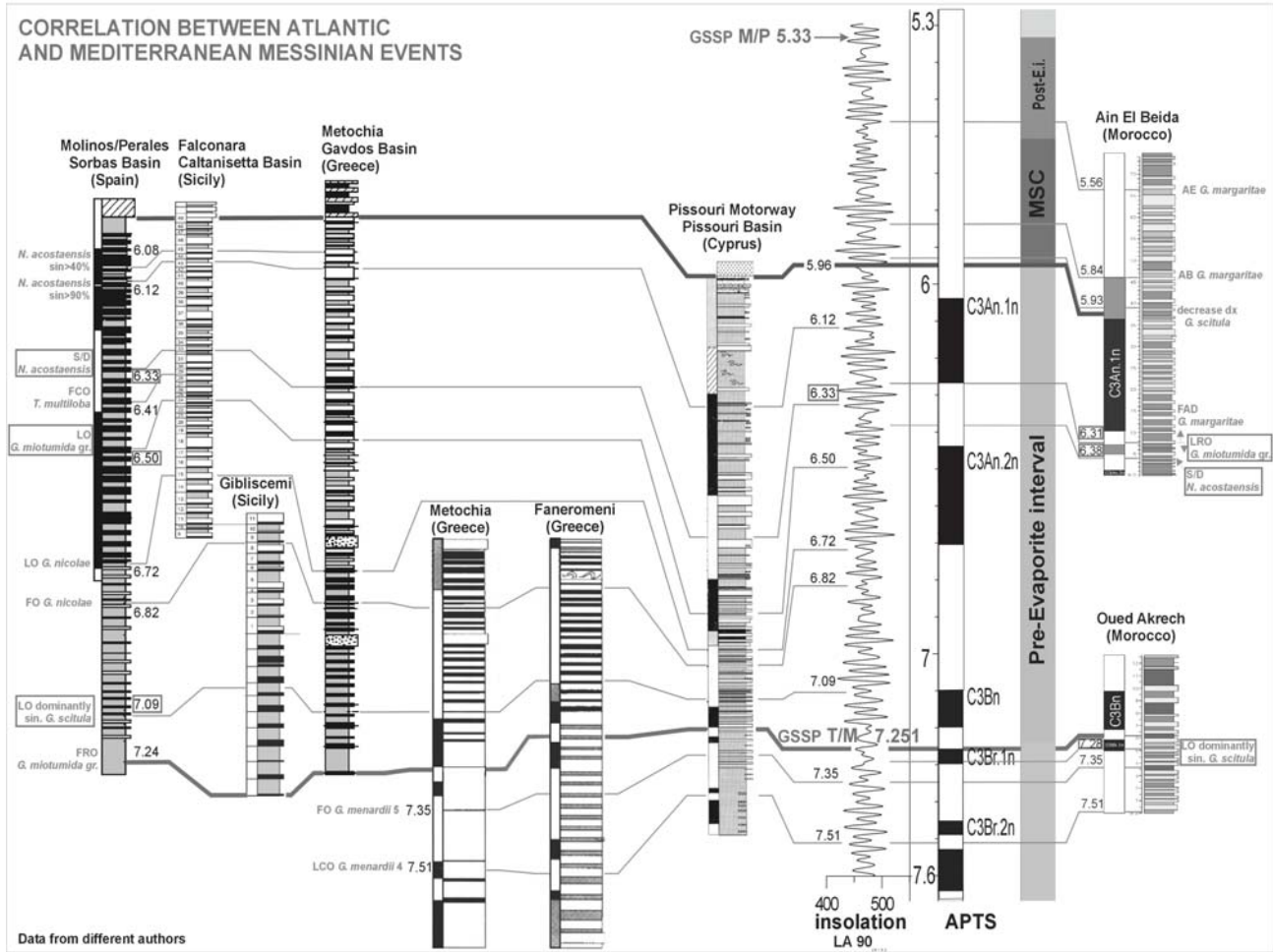
### Implications for the Messinian salinity crisis

Now that we have established a reliable and accurate time frame for the Ain el Beida section, we are able to compare the high-resolution  $\delta^{18}\text{O}$  record of AEB to  $\delta^{18}\text{O}$  records from both the Mediterranean Sea and the open ocean (text-fig. 6). This is crucial for establishing the possible link between the obliquity (41 kyr) controlled glacial  $\delta^{18}\text{O}$  cycles in the late Miocene (Hodell et al. 1994, Hodell et al. 2001, Shackleton and Crowhurst 1997, Shackleton et al. 1995a, Shackleton et al. 1995b, Vidal et al. 2002) and the initiation and ending of the Messinian Salinity Crisis in the Mediterranean in terms of glacio-eustatic sea level changes. The dominance of obliquity-scale variations in  $\delta^{18}\text{O}$  in the area of Ain el Beida was already demonstrated by Hodell et al. (1994), and has recently been confirmed in detail by spectral analysis (Van der Laan et al. 2004). By contrast, the cyclic variations in the Mediterranean marls and evaporites are dominated by precession (Hilgen et al. 1995, Krijgsman et al. 2001, Sierro et al. 1999).



TEXT-FIGURE 6

Tuning of the Ain el Beida color cycles to the 65°Nlat summer insolation and precession curves of solution La93(1,1). In addition, the combined ETP (Eccentricity, Tilt (obliquity), and negative Precession) curve is shown for comparison with the  $\delta^{18}\text{O}$  record from AEB (see van der Laan et al. 2004 for all details). Grey lines represent curves based on the new La2003(1,1) solution (Laskar et al. 2003) and reveal minor differences with the curves of the La93(1,1) solution (see also table 1). Lithostratigraphic units of the Mediterranean Messinian and their ages are indicated in columns on the right side of the figure and are based on Krijgsman et al. (1999) and Krijgsman et al. (2001). UE stands for Upper Evaporites and Zo. for Zorreras Member.



TEXT-FIGURE 7  
Correlation between the Atlantic events in sections Ain el Beida/Oued Akrech (Morocco) and the Mediterranean events in sections Molinos/Perales (Spain), Gibliscemi/Falconara (Sicily), Metochia/Faneromeni (Greece) and Pissouri (Cyprus). For detailed information about these sections the reader is referred to (Hilgen et al. 1995, Hilgen et al. 2000, Krijgsman et al. 1999a, Krijgsman et al. 2002)

The astronomical tuning of Ain el Beida immediately allows a detailed comparison of the benthic  $\delta^{18}\text{O}$  record with the  $\delta^{18}\text{O}$  records of Salé (Hodell et al. 1994), ODP Site 846 (Shackleton et al. 1995a, Shackleton et al. 1995b) from the eastern equatorial Pacific, ODP Site 926 (Shackleton and Crowhurst 1997) at Ceara Rise in the equatorial Atlantic and ODP Site 982 (Hodell et al. 2001) in the North Atlantic (see Van der Laan et al. (2004) for a review). The most pronounced glacial stages (with  $\delta^{18}\text{O}$  values of 3.2 to 3.4 ‰) in these open ocean records are TG 22 and TG 20 as well as TG 12 (coding after Shackleton et al. 1995b), which can be relatively easily identified at AEB (text-fig. 6). Various authors have linked the occurrence of peak glacials TG 22 and 20, which would imply sea level falls in the order of 50m, to the onset of the Messinian evaporites in the Mediterranean (e.g. Clauzon et al. 1996, Kastens 1992, Shackleton et al. 1995b). However, the astronomically derived ages of 5.79 and 5.75 Ma (La93(1,1)) for the peak glacial stages TG 22 and TG 20 at AEB clearly postdate the onset of the MSC (text-fig. 6), which is astronomically dated at  $5.96 \pm 0.02$  Ma (Krijgsman et al. 1999a), by approximately 200 kyr. Hence, the sea level falls associated with these glacial stages cannot be the prime cause for the onset of the MSC. In addition, no comparable glacial event associated with a prominent  $\delta^{18}\text{O}$  excursion

around 5.96 Ma can be observed at Ain el Beida. This suggests a dominantly tectonic control on the isolation of the Mediterranean Sea from the open ocean resulting in the deposition of vast amounts of evaporites, probably with a superimposed effect of the ~400 kyr eccentricity cycle which reaches a minimum just before 5.96 Ma (text-figs. 6 and 7). This conclusion was recently also reached by Hodell et al. (2001) who compared the ODP Site 982  $\delta^{18}\text{O}$  record with the Salé record and by Vidal et al. (2002) based on ODP Site 1085 in the SE Atlantic. These similar conclusions based on independent records provide important evidence that correlations between the onset of the MSC evaporites and glacio-eustatic peaks are definitely no longer acceptable. The ending of the MSC (at 5.33 Ma) can unfortunately not be documented in the stratigraphic record of the Ain el Beida section because the youngest exposed cycle has an age of 5.52 Ma (text-fig. 6). Nevertheless, it has been shown earlier that there is no single “event” in the  $\delta^{18}\text{O}$  record that corresponds to the end of the MSC and the reflooding of the Mediterranean (Hodell et al. 2001).

The only significant change in the  $\delta^{18}\text{O}$  records that seems to correspond with a major MSC-event is the peak glacial stage TG12 at 5.55 Ma (text-fig. 6). The transition from TG12 to

TABLE 2

Stratigraphic position, cycle position and astronomical ages of calcareous plankton events and magnetic reversal boundaries in section Ain el Beida. Astronomical ages are presented both for the La93(1,1) and La2003(1,1) solution.

Species/reversal	Event	Strat. range (m)	Age range (Ma)	Age range (Ma)
<b>Planktonic foraminifera</b>				
<i>G. margaritae</i>	top acme	66.80 - 67.15	5.561 - 5.558	5.560 - 5.557
<i>G. margaritae</i>	bottom acme	46.02 - 46.11	5.845 - 5.843	5.843 - 5.841
<i>G. scitula</i>	decrease dex	38.95 - 39.15	5.931 - 5.929	5.930 - 5.928
<i>G. miotumida</i>	LRO	7.73 - 7.87	6.311 - 6.309	6.309 - 6.308
<i>G. margaritae</i>	FO	7.32 - 7.57	6.315 - 6.312	6.314 - 6.311
<i>N. acostaensis</i>	sin/dex	3.99 - 4.21	6.380 - 6.375	6.378 - 6.373
<b>Calcareous nannofossil</b>				
<i>D. quinqueringus</i>	LO	68.20 - 68.50	5.548 - 5.545	5.547 - 5.544
<i>D. surculus</i>	FCO	66.47 - 66.80	5.566 - 5.561	5.564 - 5.560
<i>D. quinqueringus</i> (>20)	LO	39.66 - 39.96	5.923 - 5.920	5.922 - 5.919
<i>D. neorectus</i> (> 20)	LO	37.82 - 38.13	5.945 - 5.941	5.944 - 5.940
<i>C. mediaperforatus</i>	LCO	35.34 - 35.79	5.972 - 5.968	5.970 - 5.966
<i>A. amplificus</i>	LO	34.83 - 35.10	5.976 - 5.973	5.975 - 5.972
<i>D. quinqueringus</i>	LCO	20.01 - 20.31	6.166 - 6.163	6.166 - 6.163
<i>A. amplificus</i>	LRO	15.85 - 16.12	6.208 - 6.205	6.207 - 6.204
<i>C. macintyreii</i> (>11)	FRO	15.85 - 16.12	6.208 - 6.205	6.207 - 6.204
<i>D. quinqueringus</i>	top acme	8.92 - 9.16	6.298 - 6.296	6.297 - 6.295
<i>R. rotaria</i>	LCO	1.43 - 1.62	6.435 - 6.431	6.434 - 6.430
<b>Magnetic reversal</b>				
C3An.1n (y)	N>R	28.81 - 32.11	6.041 - 5.999	6.040 - 5.998
C3An.1n (o)	R>N	10.51 - 10.71	6.282 - 6.279	6.281 - 6.278
C3An.2n (y)	N>R	1.05 - 1.28	6.443 - 6.438	6.443 - 6.438

TG11 that marks the end of the high-amplitude, glacial-interglacial cycles of the latest Miocene (Hodell et al. 2001) roughly correlates with the base of the Upper Evaporites in the Mediterranean dated approximately at 5.52 Ma (Krijgsman et al. 2001). This implies that the Lago Mare facies of the Upper Evaporites, which was deposited when the Mediterranean was largely isolated from the Atlantic, corresponds to times of relatively high global sealevel stands and a warmer global climate than that of older parts of the Messinian.

## CONCLUSIONS

We have established a high-resolution integrated stratigraphy for the Ain el Beida section of Atlantic Morocco by applying a multi-disciplinary approach that included cyclostratigraphy, biostratigraphy (planktonic foraminifera and calcareous nannofossils), magnetostratigraphy, and stable isotope ( $\delta^{18}\text{O}$ ) stratigraphy. The 44 sedimentary cycles in Ain el Beida consist of alternating beige and reddish colored marls and reveal marked changes in thickness on a one to five to twenty ratio, which is commonly observed in sedimentary records where both precession and eccentricity play a role. The planktonic foraminiferal analyses allowed the recognition of five events, the calcareous nannofossil results revealed eight important and ten additional bioevents. They all confirm the late Messinian age of the section. Thermal demagnetization of the magnetic signal shows that three polarity reversals are recorded at Ain el Beida, corre-

sponding to chron C3An. The benthic oxygen isotope record shows a close link to the lithology with enrichments in  $\delta^{18}\text{O}$  generally occurring in the beige layers and depletions in the reddish intervals. The three heaviest peak values in  $\delta^{18}\text{O}$  are observed in beige layers in the upper part of the section.

The average periodicity of the sedimentary cyclicity, using the paleomagnetic reversals as time constraints, is 18-19 kyr, which is in good agreement with a precessional control. Detailed quantitative planktonic foraminiferal analyses and stable isotope records reveal maxima in *Globigerinoides* spp. and minima in  $\delta^{18}\text{O}$  in the reddish layers. This implies that the reddish intervals are equivalents of the sapropels in the Mediterranean and that they thus correspond to precession minima and insolation maxima. The astronomical calibration of the Ain el Beida section started with the tuning of clusters of sedimentary cycles to eccentricity, followed by the tuning of individual cycles to precession and insolation. Our calibration shows that the section comprises the time interval between 6.47 and 5.52 Ma and results in accurate astronomical ages for all sedimentary cycles, bioevents and magnetic reversals. Comparison with the Mediterranean APTS confirms that the revised astrochronology of Ain el Beida is basically correct. This allows a detailed comparison of the Ain el Beida  $\delta^{18}\text{O}$  record with Mediterranean event stratigraphy. The pronounced glacial stages TG 22 and TG 20, which have earlier been linked to the onset of the Messinian evaporites in the Mediterranean, clearly postdate the first

evaporite cycle by approximately 200 kyr. Moreover, there is no evidence at all for a glacio-eustatic control for the onset of the MSC. The only significant change in the  $\delta^{18}\text{O}$  record that corresponds with a major MSC-event is the peak glacial stage TG12 at 5.55 Ma, which roughly correlates to the transition from marine evaporites to the brackish water deposits with typical Lago Mare facies in the Mediterranean.

#### ACKNOWLEDGMENTS

We gratefully thank Dr. M. Dahmani of the 'Ministère de l'Énergie et des Mines' in Rabat for his very helpful collaboration and Dick Benson, Laura Bissoli, Krana Rakic el Bied, and Giuliana Villa (sorry for that unexpected rain cloud) for their help in the field. We furthermore acknowledge the useful comments of the reviewers W.A. Berggren and D.V. Kent. Ragna Meijer did most of the paleomagnetic measurements. This study was partly supported by the Earth and Life Sciences Research Council (ALW) of the Netherlands Organisation for Scientific Research (NWO) and was carried out under the programs of the Vening Meinesz Research School of Geodynamics (VMSG) and the Netherlands Research School of Sedimentary Geology (NSG).

#### REFERENCES

- BACKMAN, J. and RAFFI, I., 1997. Calibration of Miocene nannofossil events to orbitally tuned cyclostratigraphies from Ceara Rise. *Proceedings of the Ocean Drilling Project Scientific Results*. College Station, TX: Ocean Drilling Program. pp. 83-99.
- BENSON, R.H., HAYEK, L.A.C., HODELL, D.A. and RAKIC-EL BIED, K., 1995. Extending the climatic precession curve back into the late Miocene by signature template comparison. *Paleoceanography*, 10(1): 5-20.
- BENSON, R.H. and RAKIC-EL BIED, K., 1996. The Bou Regreg section, Morocco: Proposed Global Boundary Stratotype Section and Point of the Pliocene. *Notes et Mémoires du Service géologique, Maroc*, 383: 51-150.
- BENSON, R.H., RAKIC-EL BIED, K. and BONADUCE, G., 1991. An important current reversal (influx) in the Rifian corridor (Morocco) at the Tortonian-Messinian boundary: the end of Tethys Ocean. *Paleoceanography*, 6: 164-192.
- BOSSIO, A., RAKIC-EL BIED, K., GIANELLI, L., MAZZEI, R., RUSSO, A. AND SALVATORINI, G., 1976. Correlation de quelques sections stratigraphiques du bassin Méditerranéen sur la base des Foraminifères planktoniques. *Atti Soc. Tosc. Sci. Nat. Mem., Ser. A*, 83: 121-137.
- BUKRY, D., 1973. Low-latitude coccolith biostratigraphic zonation. *Initial Reports of the Deep Sea Drilling Project*, 15, 685-703. Washington, DC: US Government Printing Office.
- CANDE, S.C. and KENT, D.V., 1995. Revised calibration of the Geomagnetic Polarity Time Scale for the Late Cretaceous and Cenozoic. *Journal of Geophysical Research*, 100: 6093-6095.
- CITA, M.B. and RYAN, W.B.F., 1978. The Bou Regreg section of the Atlantic coast of Morocco. Evidence, timing and significance of a late Miocene regressive phase. *Rivista Italiana Paleontologia*, 84: 1051-1082.
- CLAUZON, G., SUC, J.P., GAUTIER, F., BERGER, A. and LOUTRE, M.F., 1996. Alternate interpretation of the Messinian salinity crisis: Controversy resolved? *Geology*, 24: 363-366.
- FEINBERG, H. and LORENZ, H.G., 1970. Nouvelles données stratigraphiques sur le Miocène supérieur et le Pliocène du Maroc Nord Occidental. *Notes et Mémoires du Service géologique, Maroc*, 30: 21-26.
- GARTNER, S., 1992. Miocene nannofossil chronology in the North Atlantic, DSDP Site 608. *Marine Micropaleontology*, 18: 307-313.
- HILGEN, F.J., 1991. Astronomical calibration of Gauss to Matuyama sapropels in the Mediterranean and implication for the Geomagnetic Polarity Time Scale. *Earth and Planetary Science Letters*, 104, 226-244.
- HILGEN, F.J., BISSOLI, L., IACCARINO, S., KRIJGSMAN, W., MEIJER, R., NEGRI, A. and VILLA, G., 2000. Integrated stratigraphy and astrochronology of the Messinian GSSP at Oued Akrech (Atlantic Morocco). *Earth and Planetary Science Letters*, 182: 237-251.
- HILGEN, F.J. and KRIJGSMAN, W., 1999. Cyclostratigraphy and astrochronology of the Tripoli diatomite Formation (pre-evaporite Messinian, Sicily, Italy). *Terra Nova*, 11: 16-22.
- HILGEN, F.J., KRIJGSMAN, W., LANGEREIS, C.G., LOURENS, L.J., SANTARELLI, A. and ZACHARIASSE, W.J. (1995). Extending the astronomical (polarity) time scale into the Miocene. *Earth and Planetary Science Letters*, 136, 495-510.
- HODELL, D.A., BENSON, R.H., KENNETT, J.P. and RAKIC-EL BIED, K., 1989. Stable isotope stratigraphy of latest Miocene sequences in northwest Morocco: the Bou Regreg section. *Paleoceanography*, 4: 467-482.
- HODELL, D.A., BENSON, R.H., KENT, D.V., BOERSMA, A. and RAKIC-EL BIED, K., 1994. Magnetostratigraphic, biostratigraphic, and stable isotope stratigraphy of an Upper Miocene drill core from the Salé Briqueterie (northwest Morocco): A high-resolution chronology for the Messinian stage. *Paleoceanography*, 9: 835-855.
- HODELL, D.A., CURTIS, J.H., SIERRO, F.J. and RAYMO, M.E., 2001. Correlation of late Miocene to early Pliocene sequences between the Mediterranean and North Atlantic. *Paleoceanography*, 16: 164-178.
- HSŪ, K.J., RYAN, W.B.F. and CITA, M.B., 1973. Late Miocene desiccation of the Mediterranean. *Nature*, 242: 240-244.
- KAENEL, E. DE, and VILLA, G., 1996. Oligocene-Miocene calcareous nannofossil biostratigraphy and paleoecology from the Iberia abyssal plain. *Proceedings of the Ocean Drilling Program, Scientific Results*. College Station, TX: Ocean Drilling Program 149, 79-145.
- KASTENS, K., 1992. Did a glacio-eustatic sealevel drop trigger the Messinian salinity crisis? New evidence from ODP Site 654 in the Tyrhenian Sea. *Paleoceanography*, 7: 333-356.
- KNAPPERTSBUSCH, M., 2000. Morphologic evolution of the coccolithophorid *Calcidiscus leptoporus* from the early Miocene to Recent. *Journal of Paleontology*, 74: 712-730.
- KRIJGSMAN, W., FORTUIJN, A.R., HILGEN, F.J. and SIERRO, F.J., 2001. Astrochronology for the Messinian Sorbas basin (SE Spain) and orbital (precessional) forcing for evaporite cyclicity. *Sedimentary Geology*, 140: 43-60.
- KRIJGSMAN, W., HILGEN, F.J., RAFFI, I., SIERRO, F.J. and WILSON, D.S., 1999a. Chronology, causes and progression of the Messinian salinity crisis. *Nature*, 400: 652-655.
- KRIJGSMAN, W., LANGEREIS, C.G., ZACHARIASSE, W.J., BOCCALETTI, M., MORATTI, G., GELATI, R., IACCARINO, S., PAPANI, G. and VILLA, G., 1999b. Late Neogene evolution of the Taza-Guercif Basin (Rifian Corridor, Morocco) and implications for the Messinian salinity crisis. *Marine Geology*, 153: 147-160.

- KRIJGSMAN, W., BLANC-VALLERON, M.M., FLECKER, R., HILGEN, F.J., KOUWENHOVEN, T.J., MERLE, D., ORSZAG-SPERBER, F. and ROUCHY, J.-M., 2002. The onset of the Messinian salinity crisis in the Eastern Mediterranean (Pissouri Basin, Cyprus). *Earth and Planetary Science Letters*, 194: 299-310.
- KRIJGSMAN, W. and TAUXE, L., 2004. Shallow bias in Mediterranean paleomagnetic directions caused by inclination error. *Earth and Planetary Science Letters*, 222: 685-695.
- LASKAR, J., ROBUTEL, P., JOUTEL, F., GASTINEAU, M., CORREIA, A.C.M. AND LEVRARD, B., 2004. A long-term numerical solution for the insolation quantities for the Earth, Astronomy and Astrophysics (submitted).
- LASKAR, J., JOUTEL, F. and BOUDIN, F., 1993. Orbital, precessional, and insolation quantities for the Earth from -20 Myr to +10 Myr. *Astronomy and Astrophysics*, 270: 522-533.
- LOURENS, L.J., HILGEN, F.J., LASKAR, J., SHACKLETON, N.J. and WILSON, D.S., 2004. The Neogene Period. In: F. Gradstein, Ogg, J. and Smith A., Ed., *A Geological Timescale 2004*, pp. (in press).
- MARTINI, E., 1971. Standard Tertiary and Quaternary calcareous nannoplankton zonation. *Proceedings II Planktonic Conference, Roma 1970, 2*, 739-785.
- MAZZEI, R., RAFFI, I., RIO, D., HAMILTON, N. and CITA, M.B., 1979. Calibration of late Neogene calcareous plankton datum planes with the paleomagnetic record of Site 397 and correlation with Moroccan and Mediterranean sections. *Initial Reports of the Deep Sea Drilling Program*, Washington, DC: US Government Printing Office, 47: 375-389.
- OKADA, H. and BUKRY, D., 1980. Supplementary modification and introduction of code numbers to the low-latitude coccolith biostratigraphic zonation (Bukry, 1973; 1975). *Marine Micropaleontology*, 5: 321-325.
- RAFFI, I. and FLORES, J.-A., 1995. Pleistocene through Miocene calcareous nannofossils from eastern Equatorial Pacific Ocean (Leg 138). *Proceedings of the Ocean Drilling Program, Scientific Results*. College Station, TX: Ocean Drilling Program, 138: 233-286.
- RAFFI, I., MOZZATO, C., FORNACIARI, E., HILGEN, F.J. and RIO, D., 2003. Late Miocene calcareous nannofossil biostratigraphy and astrochronology for the Mediterranean region. *Micropaleontology*, 49: 1-26.
- RIO, D., FORNACIARI, E. and RAFFI, I., 1990. Late Oligocene through Early Pleistocene calcareous nannofossils from Western Equatorial Indian Ocean (Leg 115). In: R.A. Duncan, J. Backman and L.C. Peterson, Eds., *Proceedings of the Ocean Drilling Program, Scientific Results*. College Station, TX: Ocean Drilling Program,
- RYAN, W.B.F., 1973. Initial Reports of the Deep Sea Drilling Project. Washington DC: U.S. Government Printing office, volume 13.
- SHACKLETON, N.J. and CROWHURST, S., 1997. Sediment fluxes based on an orbitally tuned time scale 5 Ma to 14 Ma, site 926. *Proceedings of the Ocean Drilling Program, Scientific Results*. College Station, TX: Ocean Drilling Program, 154: 69-82.
- SHACKLETON, N.J., CROWHURST, S., HAGELBERG, T., PISIAS, N.G. and SCHNEIDER, D.A., 1995a. A new Late Neogene time scale: application to leg 138 sites. *Proceedings of the Ocean Drilling Program, Scientific Results*. College Station, TX: Ocean Drilling Program, 138: 73-101.
- SHACKLETON, N.J., HALL, M.A. and PATE, D., 1995b. Pliocene stable isotope stratigraphy of Site 846. *Proceedings of the Ocean Drilling Program, Scientific Results*. College Station, TX: Ocean Drilling Program, 138, 337-355.
- SIERRO, F.J., FLORES, J.A., CIVIS, J., DELGADO, J.A.G. and FRANCES, G., 1993. Late Miocene globorotaliid event-stratigraphy and biogeography in the NE-Atlantic and Mediterranean. *Marine Micropaleontology*, 21: 143-168.
- SIERRO, F.J., FLORES, J.A. ZAMARRENO, I., VAZQUEZ, A., UTRILLA, R., FRANCES, G., HILGEN, F.J. and KRIJGSMAN, W., 1999. Messinian climatic oscillations, astronomic cyclicity and reef growth in the western Mediterranean. *Marine Geology*, 153: 137-146.
- SIERRO, F.J., HILGEN, F.J., KRIJGSMAN, W. and FLORES, J.A., 2001. The Abad composite (SE Spain): A Messinian reference section for the Mediterranean and the APTS. *Palaeogeography Palaeoclimatology Palaeoecology*, 168, 141-169.
- SPROVIERI, R., STEFANO, E. DI, CARUSO, A. and BONOMO, S., 1996. High resolution stratigraphy in the Messinian Tripoli Formation in Sicily. *Paleopelagos*, 6: 415-435.
- TAKAYAMA, T., 1993. Notes on Neogene calcareous nannofossil biostratigraphy of the Ontong Java Plateau and size variations of Reticulofenestra coccoliths. *Proceedings of the Ocean Drilling Program, Scientific Results*,. College Station, TX: Ocean Drilling Program, 130: 179-229.
- TAUXE, L. and KENT, D.V., 2004. A new statistical model for the geomagnetic field and the detection of shallow bias in paleomagnetic inclinations: Was the ancient magnetic field dipolar?: Timescales of the Internal Geomagnetic Field, edited by J.E.T. Channell, D.V. Kent, W. Lowrie and J. Meert, *American Geophysical Union Monograph*, (in press).
- VAN COUVERING, J.A., CASTRADORI, D., CITA, M.B., HILGEN, F.J. and RIO, D., 2000. The base of the Zanclean Stage and of the Pliocene Series. *Episodes*, 23(3): 179-187.
- VAN DER LAAN, E., GABOARDI, S., HILGEN, F.J. and LOURENS, L.J., 2004. Regional climate and glacial control on high-resolution oxygen isotope records from Ain El Beida (latest Miocene, NW Morocco): A cyclostratigraphic analysis in the depth and time domain. *Paleoceanography* (in press).
- VIDAL, L., BICKERT, T., WEFER, G. and RÖHL, U., 2002. Late Miocene stable isotope stratigraphy of SE Atlantic ODP Site 1085: Relation to Messinian events. *Marine Geology*, 180, 71-85.
- WEIJERMARS, R., 1988. Neogene tectonics in the western Mediterranean may have caused the Messinian salinity crisis and an associated glacial event. *Tectonophysics*, 148, 211-219.
- WERNLI, R., 1977. Les foraminifères planktonique de la limite mio-pliocène dans les environs de Rabat (Maroc). *Eclogae Geologicae Helvetiae*, 70, 143-191.
- YOUNG, J.R., 1990. Size variation of Neogene Reticulofenestra coccoliths from Indian Ocean DSDP cores. *Journal of Micropaleontology*, 9: 71-86.

Manuscript received November 15, 2003

Manuscript accepted August 14, 2004